*Laser and Particle Beams* (2007), *25*, 181–191. Printed in the USA.

DOI: 10.1017/S0263034607070231

# Laser ablation of ion irradiated CR-39

SHAZIA BASHIR,[1] M. SHAHID RAFIQUE,[2] AND FAIZAN UL-HAQ[1]

[1]Centre for Advanced studies in Physics, Government College University, Lahore, Pakistan
[2]Department of Physics, University of Engineering and Technology, Lahore, Pakistan

(RECEIVED 21 August 2006; ACCEPTED 13 October 2006)

**Abstract**

The effects of multiple pulses of a $CO_2$ laser with energy of 2.5 J and pulse duration of 200 ns on the surface morphology of ion irradiated CR-39 is investigated in light of the modification in its track registration properties. For this purpose, a CR-39 was exposed by a $CO_2$ laser generated hydrogen, argon, cadmium, air molecular ions ($N_2$ and $O_2$, etc.), high energy (300 KeV) proton beam from Cock Croft Walton accelerator, and $\alpha$ (5 MeV) from 0.5 $\mu$Ci $Pu^{239}$ source. The registered tracks were enlarged after 6 h of 6.25 N NaOH etching. These etched detectors were then exposed to different number of $CO_2$ laser shots. The etched detectors were then analyzed by a computer controlled optical microscope (Lexica DMR series). It was observed that even a single shot of $CO_2$ laser, irrespective of the registered ions tracks, can change the track registration properties of CR-39, and can remove the vaporization resistant skin present on the polymer (CR-39). A significant change in track density and track shaping regardless of the ions is observed. At the outside of the focal area, the ion density of different registered tracks is compared graphically before and after laser irradiation. Laser ablation of unexposed CR-39 is also done with multiple pulses $CO_2$ laser. In this regard, the coherent and non-coherent structures, diffraction patterns, circular fringes with corrugations and ripples, droplets, chain like structures with cluster formation, chain folded crystallites, and hole drilling were observed. The irradiation induced ablation of the polymer is of great importance in electronics industry, lithography, etc.

**Keywords:** Ablation; $CO_2$ laser; CR-39; Depolymerization; Ion Tracks registration

## INTRODUCTION

Ablation processes by laser interaction and the well-defined ablation of materials including polymers induced by irradiation from ultraviolet (UV), visible, and infrared (IR) lasers (Sirinivasan *et al*., 1990; Sirinivasan 1993) are of great technical interest for a variety of different applications (Beilis, 2007; Bussoli *et al*., 2007; Alti & Khare, 2006; Schade *et al*., 2006; Thareja & Sharma, 2006; Fernandez *et al*., 2005; Trusso *et al*., 2005; Rafique *et al*., 2005; Anwar *et al*., 2006), such as thin film deposition in microelectronics (Veiko *et al*., 2006), the packing industry, medicine (Wieger *et al*., 2006), photolithography, material processing including welding, cutting, patterning of materials, and biological investigation etc.

When laser interacts with polymers, a lot of phenomenon related to photothermal, photochemical, photomechanical, and photophysical processes occur. This can cause depolymerization of polymer into monomers, bond dissociation, photofragmentation, and increase in the density of chromophores, cluster formation, plasma production, and gas dynamical effects with shock waves. The entire phenomena are responsible for the change in electrical, optical, and mechanical properties of polymers, and also cause the change in the surface morphology and track registration properties of CR-39 (Miotello *et al*., 1992; Zweig & Deutsch, 1992; Himmelbaur *et al*., 1997; Korero, 1988).

Thermoset polymer of allydiglycol carbonate (CR-39) is known as an excellent material for a number of industrial, medical, and optical uses. This polymer has good optical clarity, structural stability, and resistance to heat (Kukreja & Hess, 1994). CR-39 is extensively used in various experiments in space science, nuclear science, earth sciences, fusion research, and radiation physics. Among others, one of its important uses is to characterize and identify the nature of nuclear particles. Therefore, it is very important to study how laser interaction can change the track registration properties of CR-39 during laser processing.

Most reports are related to ablation of polymers like Polymethylmethacrylate (PMMA), $\tau$, and polyethylene terephthalate (PET) with UV lasers (Sutcliff & Sirinivasan, 1986), but very little work is reported on IR laser irradiation

Address correspondence and reprint requests to: M. Shahid Rafique, Department of Physics, University of Engineering and Technology, Lahore, Pakistan. E-mail: shahidrafiq@uet.edu.pk

effects especially on track registration properties of CR-39 (Sumiyoshi *et al*., 1994; Jarad *et al*., 1993; Kukreja, 1991, Shahid *et al*., 2004).

The present work deals with the study of laser ablation of CR-39. The work also includes the study of change in the track registration properties of CR-39 after irradiation with multiple pulses of $CO_2$ laser. The registered ions are $CO_2$ laser generated hydrogen, argon, cadmium, air molecular ions ($N_2$ and $O_2$ etc.), high energy $\sim$ 300 KeV protons from the Cock Croft Walton accelerator (Centre for Advanced Studied in Physics Government College University, Lahore, Pakistan), and $\alpha$ (5 MeV) from $Pu^{239}$ source (0.5 $\mu$Ci).

## EXPERIMENTAL WORK

The experimental setup to expose ion irradiated CR-39 with transversally excited atmospheric (TEA) $CO_2$ laser is shown in Figure 1. First, the detector (1.5 $\times$ 1.5 $cm^2$ dimensions with a thickness of 0.5 cm) was exposed to forwardly peaked laser (Shahid *et al*., 2004) induced plasma ions of hydrogen, argon, and air molecular ions ($N_2$, $O_2$, etc.), under one atmospheric pressure (760 torr), and by Cd ions in $\sim 10^{-6}$ torr vacuum. For this purpose, all of the above mentioned gases were placed in a vacuum chamber at a pressure of 760 torr. After passing through the KBr transmission window, the laser was focused with Ge lens to a focal length of 15 cm. The detector was placed at an angle of 45° to the incoming laser beam. High density plasma was produced and the detector was exposed by respective ions. Another source used for irradiation of CR-39 was the Cock Croft Walton accelerator. A high energy $\sim$ 400 KeV proton beam from this accelerator was used to expose CR-39 in a vacuum ($10^{-6}$ torr). $Pu^{239}$ (0.5 $\mu$C) is used to expose the detector by 5 MeV $\alpha$-particles. After exposure with different ions, the detector was etched using 6.25 N NaOH solution maintained at 70°C for 6 h. The track diameters and track density was observed. These etched detectors were then exposed by $CO_2$ laser for different number of pulses. The energy fluence was 27.27 J/$cm^2$ with pulse duration of 200 ns. The untreated CR-39 was also directly exposed to the laser for different number of pulses at a fluence of 27.27 J/$cm^2$.

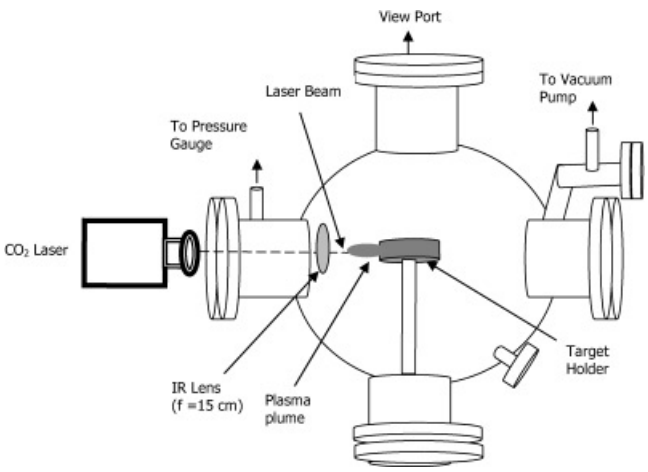


**Fig. 1.** The experimental setup for the exposure of CR-39 by TEA $CO_2$ laser.

The laser irradiation effects on track registration properties of CR-39 were observed by a computer controlled Lexica (DMR Series) optical microscope. The average track density before irradiation and after laser irradiation outside focal area was measured by stage micrometer.

## RESULTS

### Laser ablation of CR-39

Very significant ablation of CR-39 was observed after irradiation with a $CO_2$ laser at an energy level of 2.5 J by optical microscope. A significant change in the surface structure of the polymer was observed. Very interesting features have been obtained in terms of formation of diffraction pattern, surface corrugations, periodic, chain-like structures, laser-induced hydrodynamical instabilities with coherent, non-coherence structures, melting, and roughness by expulsion of liquid droplets. The dissociation of polymer into monomer due to bond breaking can be considered as a thermal ablation mechanism of polymer.

Figure 2 shows laser ablation of CR-39 with an energy level of 2.5 J per pulse. Figure 2a shows fringes and corrugations after exposure to five pulses and Figure 2b represents polymer surface after exposure to 10 pulses, with more dominant, regular fringes, and diffraction pattern. The width and clarity of fringes increases with increasing number of pulses. The diameter or widths of the first clear fringe is 1 $\mu$m after exposure to five pulses, while it increases to 10 $\mu$m after exposure to 10 pulses. These circular fringes and diffraction pattern in Figure 2 are coherent structure of the polymer. The feedback that causes coherent and non-coherent structure formation can originate from different mechanisms such as local thermal expansion, changes in optical or thermal properties, surface tension effects, surface acoustic waves, capillary waves, melting vaporization, transformation energies, and chemical reactions etc (Bauerle, 1996). In the case of strongly absorbing surfaces, the effect might be described qualitatively in the following way.

1. Interference of the incoming light wave with the wave that is reflected at the surface roughness leads to the generation of spatial grating on the surface.
2. At the position of the interference maxima, the surface is strongly heated, resulting in melting, and evaporation. Permanent grating is engraved onto the surface from which the incoming light wave is scattered. Since the corrugated surface acts as periodic dielectric wave-guide for incident radiation (Allmen, 1987).

https://doi.org/10.1017/S0263034607070231 Published online by Cambridge University Press

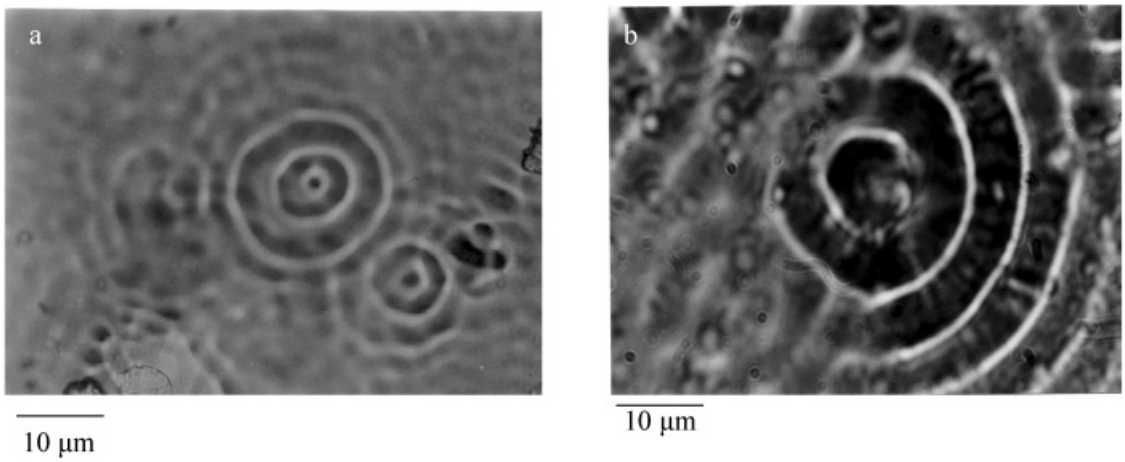


**Fig. 2.** TEA $CO_2$ Laser (2.5 J per pulse, 200 ns, and 10.6 $\mu$m wavelength) ablation of CR-39. (**a**) After exposure to five pulses with fringes and corrugations. (**b**) After exposure to 10 pulses with more dominant fringes and diffraction pattern.

This kind of positive feedback results in a strong increase in the depth of grating, until the lateral evolution of heat limits the lattice modulation by occurrence of melting processes closed to interference phenomena. Hence quality of surface grating depends very much on thermal material constants. On polymer surface grating with amplitude greater than 100 nm and period of 280 nm have been generated via irradiation with fourth harmonic of Nd:YAG laser ($\lambda$ = 266 nm) (Rubhn, 1999). Because of excellent coherence of laser irradiation it is fairly straight forward to create periodic intensity variation on the surface of the sample via two-or four-beam laser interference. The laser beam may split up into two equal parts while passing through different layers of polymer and interfere under an angle $\alpha$ on the sample surface. This gives periodic modulation of laser intensity across the period (Rubhn, 1999)

$$P = \lambda/\sin(\alpha/2),$$

where $\lambda$ is the laser wavelength. The period $P$ of the grating can be varied either by changing the laser wavelength or the interference angle $\alpha$. The intensity of the laser light varies with period $P$ as follows:

$$I = I_o \cos^2\left(\frac{\pi x}{P}\right),$$

where $x$ shows the direction of propagation of the laser beam.

Coherence structures have a common origin. The oscillating radiation field on the material surface which is generated by interference between incident laser beam and scattered/excited surface waves has fixed periodicity. The spiral periods of such structures are therefore proportional to the laser wavelength.

Noncoherence structures are not directly related to any spatial periodicity of the energy input caused by interference phenomena. Here the feedback results in either spontaneous symmetry breaking or in a non-trivial spatiotemporal ordering of the system (Gaponov *et al*., 1989; Haken, 1978; Nicolis & Prigogine, 1977).

Figure 3 shows optical micrograph after $CO_2$ laser ablation of CR-39 at pulse energy 5 J with chain-like structures and formation of clusters. Figure 3a shows the surface after exposure to five pulses and Figure 3b shows the surface after exposure to10 pulses with more pronounced chains and cluster formation. The series of chains were found on the surface of CR-39 may have been due to the high temperature produced from high energy delivered by laser pulse. This chain may be attributed to thermal spikes due to emitted atoms and molecules from extreme outer surface, and nucleation of vapor bubbles at or beneath the surface does not enter (John & Haglund, 1998). It was observed that the degree of ripples formation within these clusters of chains increases with the increase in number of pulses. The formation of these clusters of chain could be due to the adsorption effect of $CO_2$ laser where oxygen is removed from the uniform CR-39 polymer chains, and ultimately the formation of new chain structures.

From the temporal temperature profiles at the surface of the polymer, it is also noticed that the surface remains at a temperature of depolymerization for a longer period of time at 25 J/cm$^2$ than that at 9 J/cm$^2$. Although in the absence of information on the kinetics of the depolymerization and that of clustering of the depolymerization units (oligomers), it is difficult to give a precise reason for the dependence of the microstructure on the laser fluence. One possible reason could be that the time for which the surface of the polymer is at a temperature more than that for the depolymerization and therefore the oligomer clusters grow to a larger size. The large surface cooling rates (in excess of 1000°C/s), following the laser-induced depolymerization, could also play a significant role in the formation of the heterogeneous porous microstructure in the treated surface of this polymer. The oligomers formed due to the interaction of the laser with

https://doi.org/10.1017/S0263034607070231 Published online by Cambridge University Press

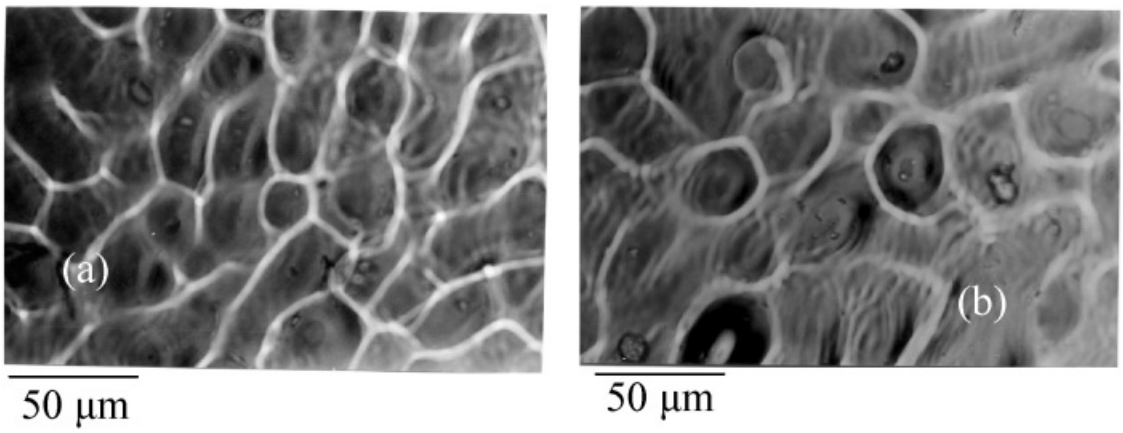


**Fig. 3.** $CO_2$ laser ablation of CR-39 at pulse energy 5 J with chain-like structures and formation of clusters. (**a**) After exposure to five pulses. (**b**) After exposure to 10 pulses.

polymer, when frozen at a rapid cooling rate, resulting in the formation of a metastable structure. This is because the oligomers do not have time to settle in the most stable state. A possible reason for the formation of the voids on microstructure surface could be that gases released during the laser heating are trapped on the rapidly cooling polymer surface. These gases could have been released either because of the photodecomposition of the polymer itself or from the occluded gases and moisture, etc., released on heating the polymer (Kukreja, 1991).

Figure 4 shows surface morphology of different ablation phenomenon on CR-39 at pulse energy 2.5 J of $CO_2$ laser. Figure 4a shows hydrodynamical sputtering after single pulse of $CO_2$. Figure 4a refers to the process in which droplets of the material are formed and are expelled from the target as a consequence of transient melting. For polymer surfaces, droplet formation was observed by Nivis *et al.* (1998). These droplets as asperities are accelerated away from the molten substrate during each pulse, owing to combination of volume change on melting followed by thermal expansion of the liquid. The ejection of species from the surface was ascribed to building up stresses related to local volume increase (Nakai *et al.*, 1991). It can be considered as a laser-cone formation mechanism. Concrete evidence suggests that vaporization resistant impurities are responsible for laser-cone formation.

Figure 4b is representing secondary ripples caused by stimulated scattering, due to surface polarization waves on the surface of CR-39, after five-pulses of the $CO_2$ laser. The scattered field from different scattering features gives rise to secondary ripples. The resulting pattern contains Fourier components at several spatial frequencies. Thus, once fringe pattern have been physically impinged on the surface, it can perpetuate itself after overlapping laser shots. The shockwaves can also cause such instabilities where surface supports excitation of plasma polarization or acoustic waves (Bauerle, 1996).

Figure 4c shows laser-induced coherent structures after five pulses and Figure 4d shows laser-induced incoherent structures after five pulses on a different focal region. Figure 5a represents chain-folded crystallites tracks on CR-39 after 10 pulses of $CO_2$ laser irradiation at an energy level of 2.5 J outside of the focal area, and Figure 5b shows holes drilled in CR-39 after 15 pulses of $CO_2$ at pulse energy 2.5 J with burning and depolymerization of polymer outside of the drilling. Chain-folded lamellar crystallites (Bower, 2002) shown in Figure 5a plays an important part in the structure of most ordinary crystalline polymers. Fold surfaces are not perfectly regular, particularly for melt-crystallized materials. Buried fold exists up to a few nm below the surface, but the number of sharp fold increases as the overall surface is reached. In melt-crystallized material, tie molecules pass from one lamellar to adjacent ones in the multilayer stacks (Bower, 2002). Figure 5b shows the phenomena of channeling of laser beam in the polymer to create holes. Deeper cavities formed by more intense beams can have interesting and beneficial consequences on beam-solid coupling. Drilling of holes requires irradiances capable of substantial surface removal. The speed of material removal increases with local irradiance and Gaussian beams tend to form round holes with diameter roughly equal to the beam diameter near the surface. Outside the drilling, burning of the polymer is clear. The basic sequence is that material melts, undergoes deformation, and finally after irradiation, resoldifies making the deformation permanent.

## Effect of laser irradiation on track registration properties of CR-39

The effect of multiple pulses of $CO_2$ laser, at 10.6 $\mu$m wavelength, energy level of 2.5 J, and pulse duration of 200 ns, on the track registration properties of CR-39 has been studied. It was observed that a single shot of $CO_2$ laser can change the track registration properties of CR-39 and can remove the vaporization resistant skin present on the polymers. The change in the track diameter, track density, and track shaping of different ions was observed. The sig-

https://doi.org/10.1017/S0263034607070231 Published online by Cambridge University Press

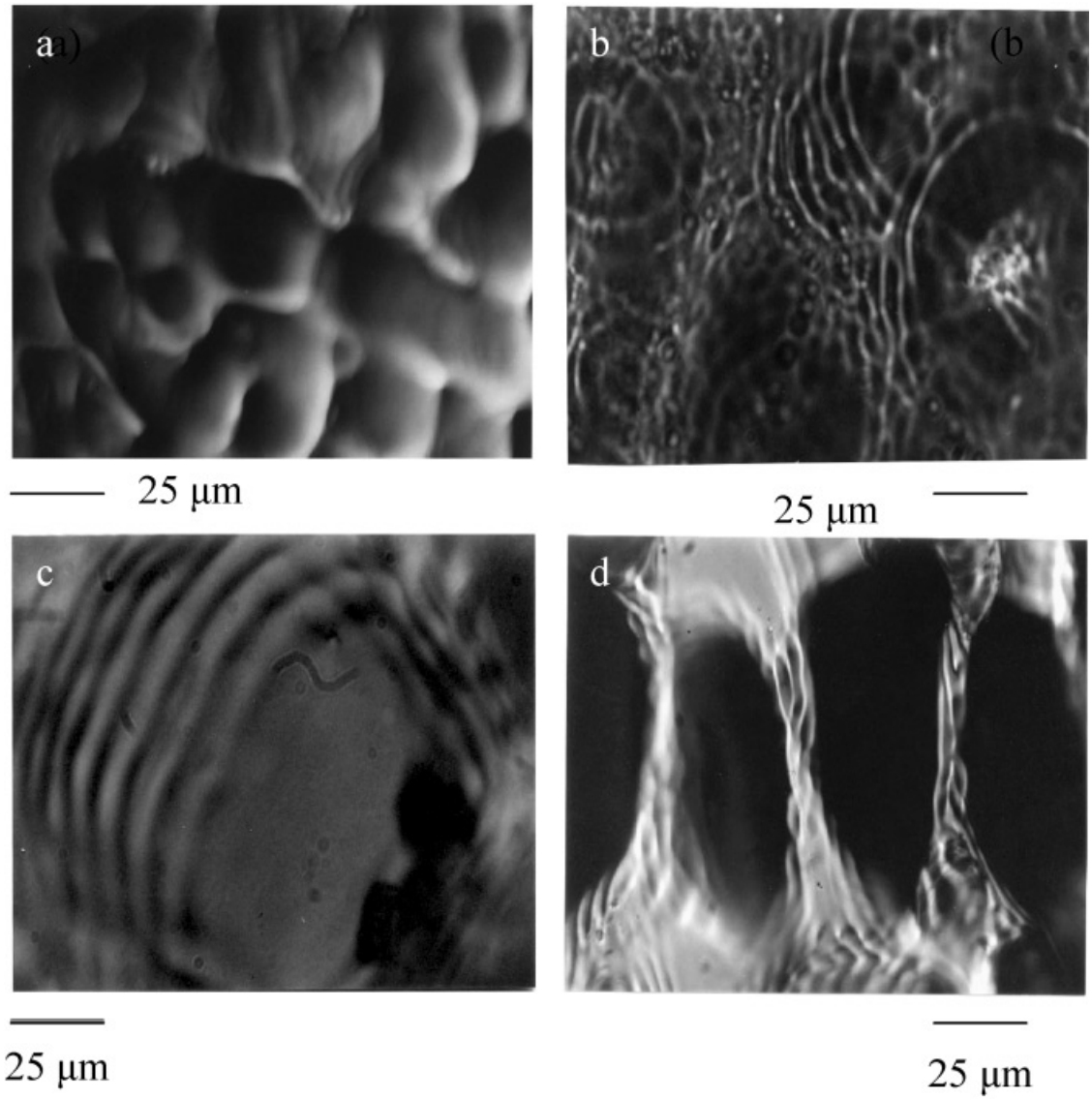


**Fig. 4.** Different ablation phenomenon in CR-39 at pulse energy 2.5 J of $CO_2$ laser. (**a**) Hydrodynamical sputtering after single pulse of $CO_2$. (**b**) Secondary ripples caused by stimulated scattering due to surface polarization waves at the surface of CR-39. (**c**) Laser-induced coherent structure after five pulses. (**d**) laser-induced incoherent structure after five pulses at different focal region.

nificant change in the track density of the tracks was attributed to registration of laser-induced plasma ions in air. The annealing of the central area of the detector was observed and this area increases with increasing number of pulses unless a rupturing of the drilling of the polymer occurs. It was also observed that surface structures of the polymer has been modified in terms of formation of diffraction pattern, chain-like structure, bubble formation, stress related instabilities with coherent and non-coherent structures, bond dissociation, increase in the density of chromophores, photofragmentation, plasma production, splashing, sputtering, melting, and burning. The change in tracks registration properties was observed by the following optical micrographs.

Figure 6a presents the untreated surface of CR-39, which has been exposed to air molecular ions ($N_2$, $O_2$). Figure 6b shows laser-induced surface melting and resolidification after laser treatment of the polymer. The particulates induced the formation of defects and reshaping of tracks. The tracks are appearing either at the center of the chains or at the boundary of the chains. Tracks density has been reduced several order at the center of the laser focus due to annealing of the polymer.

Figure 7a shows the untreated optical micrograph of tracks on laser-induced plasma ions of hydrogen at 1 atm of pressure on CR-39. Figure 7b shows the laser treated surface of CR-39. Circular tracks have been changed to hexagonal, elliptical, and triangular shapes in Figure 7b. While in Figure 7c, the broken chains and wave-like ridges formation due to coherent and non-coherent instabilities are shown. In Figure 7d, a significant change in track registrations can be

https://doi.org/10.1017/S0263034607070231 Published online by Cambridge University Press

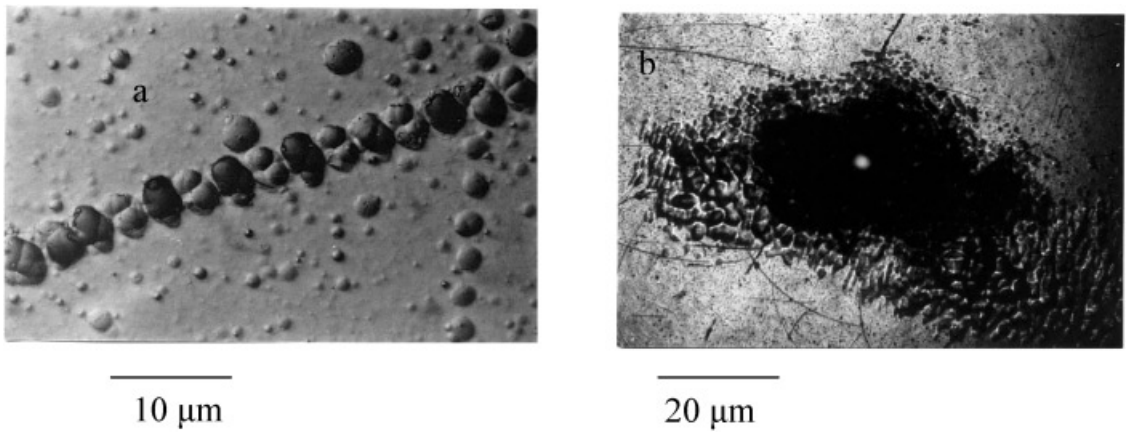


**Fig. 5.** (**a**) Chain folded crystallites with tracks on CR-39 after $CO_2$ laser irradiation with 10 pulses at pulse energy 2.5 J outside the focal area. (**b**) Hole drilling of CR-39 after 15 pulses of $CO_2$ at pulse energy 2.5 J with burning and depolymerization of polymer outside the drilling.

observed in terms of track density, track diameter, and track reshaping.

Figure 8a shows the untreated surface of CR-39 tracks of Cd ions with circular fringes and diffraction pattern. Figure 8b shows the laser treated surface of CR-39 for reshaping of Cd ions with droplet formation and surface splashing of polymer. Two boundaries are separating treated and untreated region, making a canal between the ablated and un-ablated area.

Figure 9a shows the optical micrograph of the untreated surface for the tracks of laser-induced plasma ions of argon with conical shape. Figure 9b shows the laser treated surface of CR-39. It shows reshaping of argon ions with diffraction pattern and broken chains.

Figure 10a shows untreated surface of CR-39 with tracks of 300 KeV protons produced by the Cockroft Walton accelerator with very large flux. Figure 10b shows reshaping of circular tracks of protons (300 KeV) after laser treatment

Figure 11a and Figure 11b shows the circular tracks of alpha particles on CR-39 produced by $Pu^{239}$ in a $\sim 10^{-3}$ torr vacuum and under atmospheric conditions, respectively. Figure 11c shows laser treated surface of CR-39 for reshaping of 5 MeV alpha particles produced by $Pu^{239}$ (0.5 $\mu$Ci) with photofragmentation and recondensation. No alpha tracks appear at this scanning area showing that the radiation induced skin has been removed due to laser irradiation effects.

Figure 12 gives a comparative study of density of different ions registered on CR-39 before and after treatment with $CO_2$ laser. Figure 12 shows that the density of ions is enhanced 100 times due to registration of laser-induced plasma ions of air molecules ($O_2$, $N_2$...). The scanned area was out of focal volume.

The significant change in track registration properties of CR-39 in terms of tracks size, track density, and shapes may be due to coherent, non-coherent, and hydrodynamical insta-

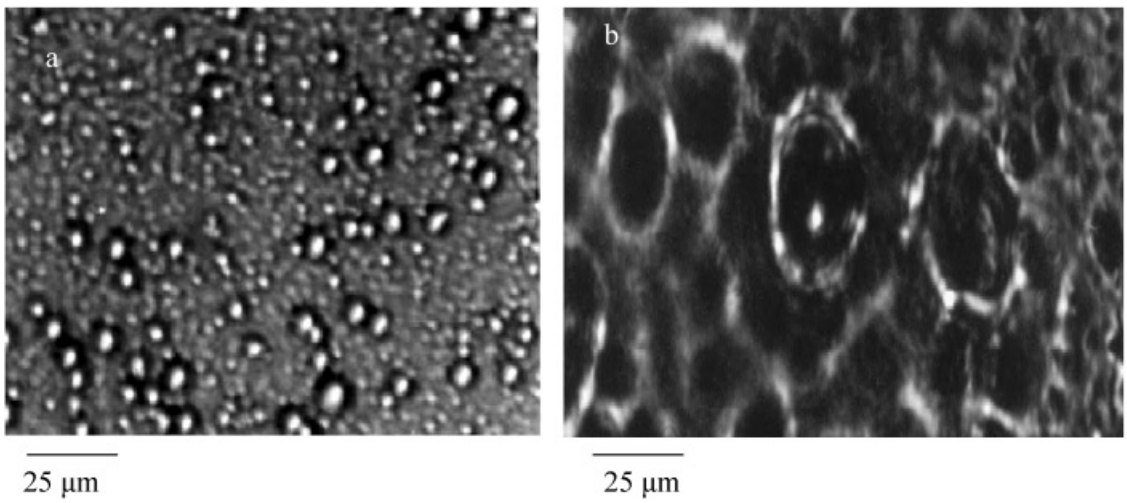


**Fig. 6.** (**a**) Laser untreated surface of CR-39 exhibiting tracks of laser-induced plasma ions of air molecules ($N_2$, $O_2$). (**b**) Laser treated surface of CR-39 for reshaping of air molecular ions ($N_2$, $O_2$).

https://doi.org/10.1017/S0263034607070231 Published online by Cambridge University Press

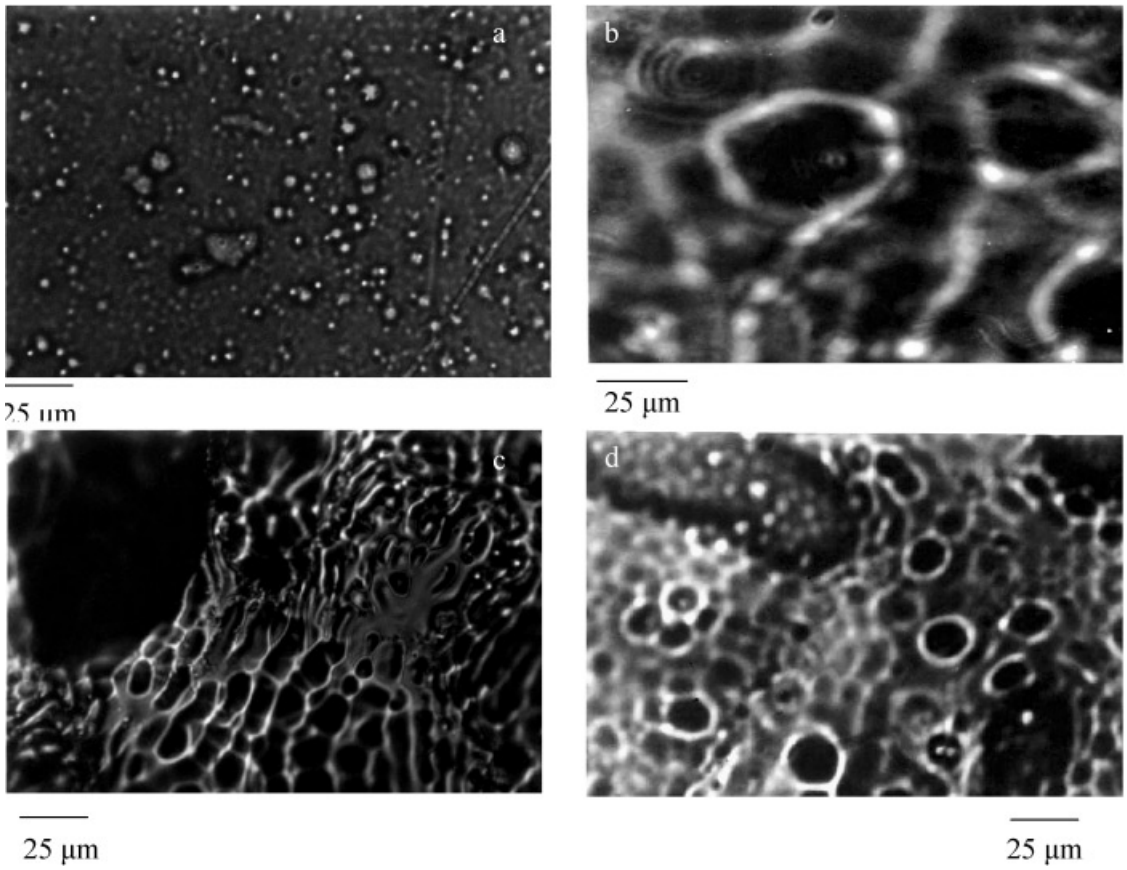


**Fig. 7.** (**a**) Laser untreated surface of CR-39. Tracks of laser-induced plasma ions of $H_2$ at 1 atm. (**b**) Laser treated surface of CR-39 for reshaping of $H_2$ ions. Surface modification has been observed and circular tracks have been changed to hexagonal, elliptical and triangular shape. (**c**) Laser treated surface of CR-39 for reshaping of $H_2$ ions. Surface modification has been observed in terms of broken chains and wave like ridges due to coherent and noncoherent instabilities. (**d**) Surface modification has been observed in terms of track density, track diameter and track reshaping

bilities. These effects may be due to shock waves produced by the high power laser. The depolymerization and fragmentation of monomers from polymer may be attributed to the thermal effect of IR irradiation. Different registered tracks have been modified after laser treatment in different ways. Because these registered tracks can then act as the defects of material and therefore enhance the electric field of the electromagnetic radiation of laser in different ways. There-

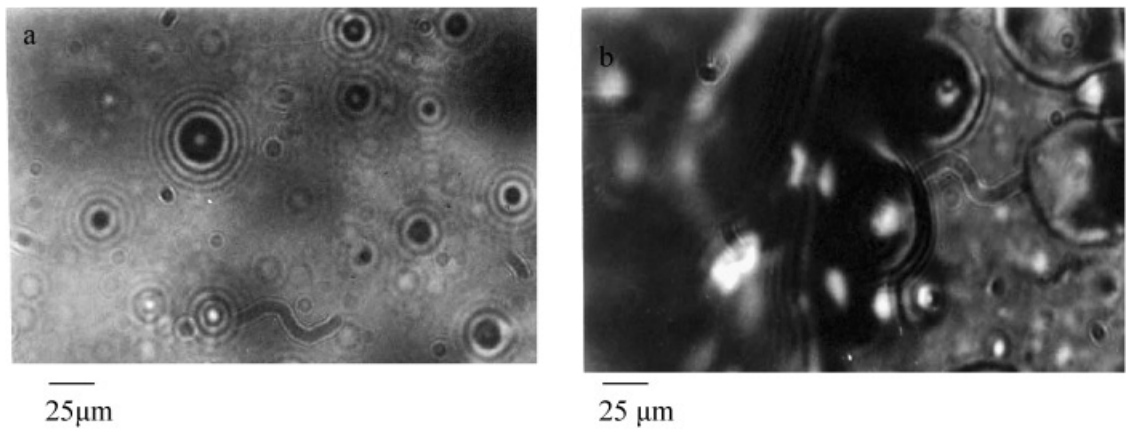


**Fig. 8.** (**a**) Untreated surface of CR-39. Tracks of Cd ions with diffraction patterns. (**b**) Laser treatment has reshaped tracks of Cd ions. Bubble formation with melting boundary (Knudsen layer) is also clear.

https://doi.org/10.1017/S0263034607070231 Published online by Cambridge University Press

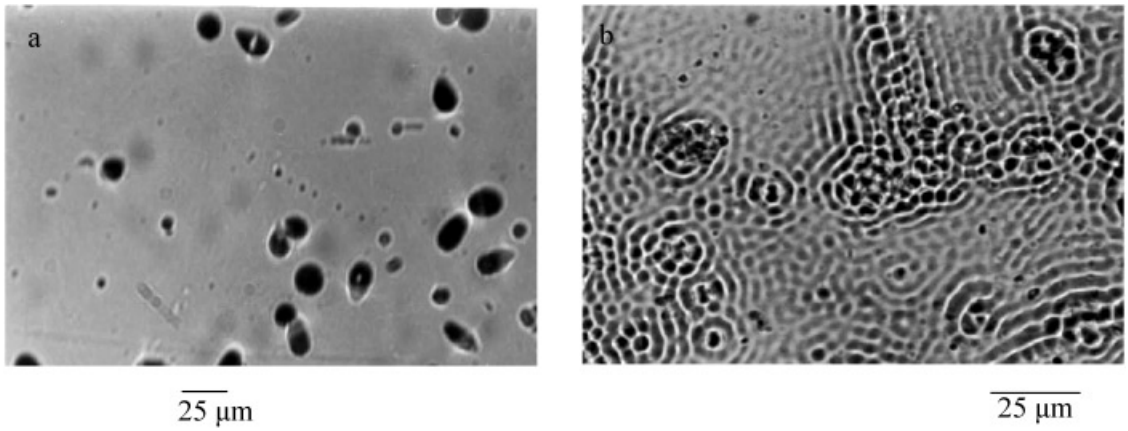


**Fig. 9.** (**a**) Optical micrograph of untreated surface of CR-39 with conical tracks of laser-induced plasma ions of argon at 1 atm (760 torr). (**b**) Optical micrograph of laser treated surface of CR-39 with reshaping of the tracks of argon ions with diffraction pattern and broken chains.

fore, they cause different surface structures due to the difference in the absorption of laser radiation. The diffraction pattern originates from the interference between the incident laser light and scattered excited wave along the interface. Scattering of incident light can be caused by the microscopic roughness of the surface due to defects produced by tracks of different ions. The interference between the incident and scattered radiation field leads to inhomogeneous energy input which in turn cause surface instabilities.

Laser-induced photofragmentation can change the bond energy. The particulates and globules induced defects can also reshape the tracks. Electronic excitation increases the density of chromophores and enhances the multiphoton band gap excitation. This will alter the binding energies of the neighboring atoms and their coupling to crystal lattice. These electrons can increase the total energy by an amount similar to $N_e E_{gap}/N$ where $E_{gap}$ is the energy gap and $N$ is the density of the target atom (John & Haglund, 1998). As in CR-39, there are 39 atoms in one molecule of $C_{12}H_{18}O_9$. So there are 3N-6 = 111 modes of vibrations. Hence, the average electron energy per irrational mode is distributed by 39 atoms and 111 modes. The average energy per irrational mode (Duley, 1996) at the threshold is then

$$\eta_T = \frac{\sigma n_c F_T \hbar\omega}{(3N-6)} = \frac{\sigma n_c F_T \hbar\omega}{111},$$

where $\sigma$ is the cross-section per chromophore ($\sigma = (\alpha/N_c)$), $\alpha$ is the absorption coefficient, and $N_c$ is the number of chromophores per $cm^3$, $n_c$ is the number of chromophores per monomer, $\hbar\omega$ is the incident photon energy, $F_T$ is the threshold photon fluence (photon $cm^{-2}$). The threshold fluence (Duley, 1996) is therefore,

$$E_T = F_T \hbar\omega.$$

By substituting the approximate values typical of a polymer (Duley, 1996), $\sigma = 2 \times 10^{-17}$ $cm^2$, $N_c = 10^{22}$ $cm^{-3}$ from $N_c = n_c N_m$, with $N_m$ as the density of monomers, taking $N_m =$

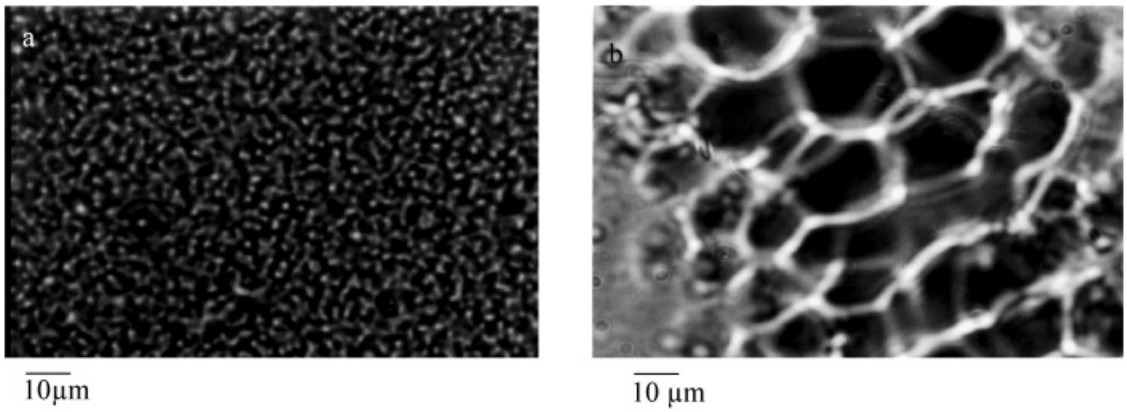


**Fig. 10.** (**a**) Untreated surface of CR-39 with tracks of protons at 300 KeV produced by Cockroft Walton accelerator with very large flux. (**b**) Reshaping of circular tracks of protons (300 KeV) after laser irradiation with burning and depolymerization with few larger tracks.

https://doi.org/10.1017/S0263034607070231 Published online by Cambridge University Press

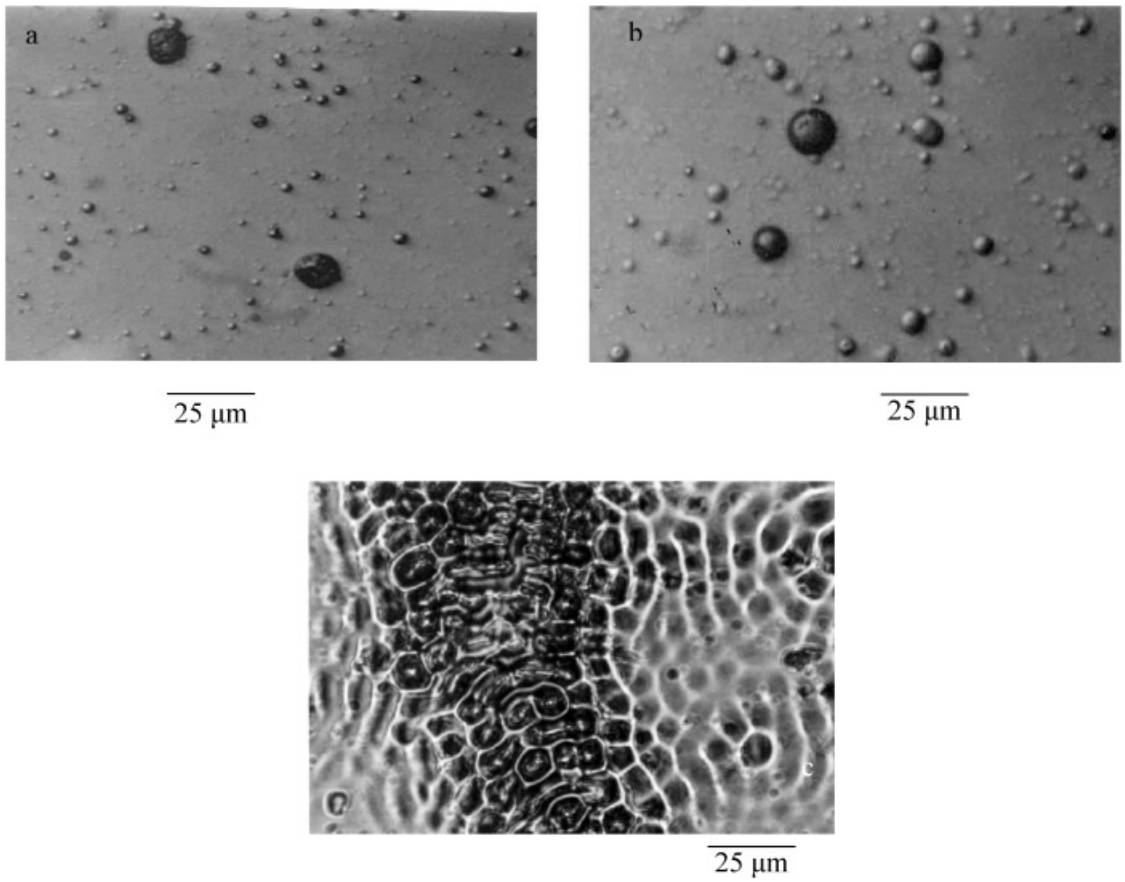


**Fig. 11.** Surface of CR-39 with circular tracks of alpha particles produced by $Pu^{239}$. (**a**) Under vacuum $\sim 10^{-3}$ torr. (**b**) Under atmospheric conditions. (**c**) Laser treated surface of CR-39 for reshaping of alpha particles produced by $Pu^{239}$ with photofragmentation of the material.

$10^{21}$, $n_c$ comes out to be 10, $\sigma n_c$ comes out to be $2 \times 10^{-16}$. By substituting the calculated value of the threshold fluence (0.001 J/cm$^3$), we get irrational energy of 0.0112 eV per mode.

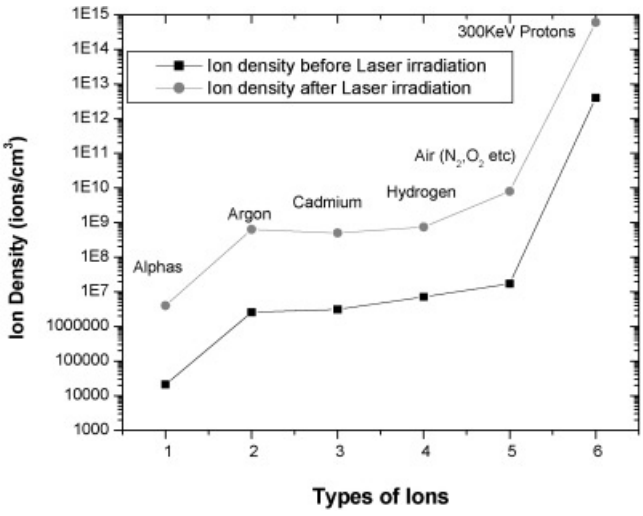


**Fig. 12.** The comparative study of density of different ions registered on CR-39 before and after its treatment with $CO_2$ laser.

Basically the tracks behave like defects and impurities. The defects at the surface intensify the electric field of incident laser. Thus, the distribution of laser energy to the vibration energy per mode of polymer will be enhanced, and this can enhance the ablation rate of the polymer. As the tracks behave like defects and plays several important roles in laser-induced desorption. First, they change the electronic structure of the surface and near surface bulk material by generating states in the band-gap, and hence they alter the local optical response of the solid. Second, defects represent sites that have different charge, binding, and electronic structure than perfect sites in the bulk lattice. Third, they can alter the vibration response of the solid by generating localized modes. In any case, the alteration have significant effect on desorption. Damage threshold can vary greatly within one particular sample due to compositional variation, localized imperfections, and absorption centers. This is the main reason that after track registration, less energy may be dissipated in ablation of CR-39.

The vibration frequencies and lifetime of the defected states may be enhanced compared to those of ordinary atoms at non-defected sites (Page, 1974). This is because the defected site does not couple efficiently to the harmonic bath of phonons in the solid; hence, vibration excitation in

https://doi.org/10.1017/S0263034607070231 Published online by Cambridge University Press

these states may be slow and randomized by cooling transitions (Bicham & Sievers, 1991).

If the released energy $E_{ex}$ is converted completely into kinetic energy of the evaporating molecules, then the fragments should have a velocity of (Rubhn, 1999)

$$v = \sqrt{\frac{2E_{ex}}{m}}.$$

Here $m$ is the mass of the molecular fragments and

$$E_{ex} = E_{ph} - E_B,$$

with photon energy $E_{ph}$, and binding energy $E_B$. Photodegradation occurs when an incident photon is absorbed by a chromophore or covalently unsaturated molecular group (that is, C=C, C=O, etc.). This electronically excited group may dissociate immediately and undergoes reaction with another molecular entity, or retains some or all of the initial energy as electronic/vibrational excitation. Direct bond breaking can lead to the evolution of the gas and formation of the radicals within the irradiated volume. It is the rapid evolution of the gas that is responsible for the clean edges associated with photoablation phenomena.

In dielectrics or polymers, the free carriers are absent and absorption of photon below band-gap radiation takes place inside of the lattice. As laser beam impinges on the surface forming a molten layer. This layer is referred to as a Knudsen layer (John & Haglund, 1998), as can be observed in Figure 8b. The vaporization process which takes place in a very short time but with a considerable amount of mass transport exerts a recoil pressure. Cain *et al*. (1992) adopted a pure photothermal description of the ablated process in which absorbed photon energy is converted into heat, which then drives a thermal degradation waves into the polymer. The position of the surface is given by Duley (1996)

$$\frac{ds}{dt} = k_o \exp\left[-\frac{\varepsilon}{(kT)}\right].$$

Where $\boldsymbol{k_o}$ is the Arrhanius factor, $\varepsilon$ is the activation energy, and $\boldsymbol{k}$ is the Boltzmann's constant. On a molecular basis, weak bonds are the first to be broken leading to the evolution of molecular fragments. The parent molecule then undergoes a rearrangement or a reaction with its environment to yield a product with fewer bonds that are susceptible to dissociation under ambient radiative conditions.

## CONCLUSION

From the results obtained above, it can be inferred that laser has modified the surface morphology, degree of crystallinity, chemical composition, and sensitivity of the polymer surface. The photothermal ablation is dominant mechanism in which absorbed photon energy is converted into heat which then drives a thermal degradation waves into the polymer. This photothermal ablative process is leading to photofragmentation, depolymerization, and cluster formation. Very interesting features have been obtained in terms of formation of diffraction pattern, surface corrugations, periodic, and chain-like structures, laser-induced hydrodynamical instabilities with coherent, non-coherence structures, melting, and roughness with expulsion of liquid droplets. Significant changes are produced in the track registration properties of CR-39 regarding track reshaping, track diameters, and track density. Some circular tracks have been changed to hexagonal, elliptical, and triangular shapes, while in some cases, the broken chains and wave-like ridges formation due to coherent and non-coherent instabilities appeared on the surface of ion irradiated CR-39. The droplet and bubble formation, surface splashing, and diffraction patterns with annealing of are also present after laser treatment of ion irradiated CR-39. Different registered tracks have been modified after laser treatment in different ways. Because these registered tracks can then act as the defects of polymer, and therefore enhance the electric field of the electromagnetic radiation of laser in different ways. The enhancement in the multiphoton band-gap excitation will cause change in the bond energy and average vibrational energy per mode.

## REFERENCES


Allmen, M.V. (1987). *Laser-Beam Interactions with Materials*. New York: Springer-Verlag.

Alti, K. & Khare, A. (2006). Low-energy low-divergence pulsed indium atomic beam by laser ablation. *Laser Part. Beams* **24**, 47–53.

Anwar, S.M., Latif, A., Iqbal, M., Rafique, S.M., Khaleeq-ur-Rahman, M. & Siddique, S. (2006). Theoretical model for heat conduction in metals during ultra short laser pulse. *Laser Part. Beams* **24**, 347–353.

Bauerle, D. (1996). *Laser Processing and Chemistry*. New York: Springer-Verlag.

Beilis, I.I. (2007). Laser plasma generation and plasma interaction with ablative target. *Laser Part. Beams* **25**, 53–63.

Bicham, S.R. & Sievers, A.J. (1991). Intrinsic localized modes in a monatomic lattice with weakly anharminc nearest-neighbour force constants. *Phys. Rev. B* **43**, 2339–2346.

Bower, D.I. (2002). *An Introduction to Polymer Physics*. Cambridge, UK: Cambridge University Press.

Bussoli, M., Batani, D., Desai, T., Canova, F., Milani, M., Trtica, M., Gakovic, B. & Krouski, E. (2007). Study of laser induced ablation with fib devices. *Laser Part. Beams* **25**, 121–125.

Cain, S.R., Burns, F.C., Otis, C.E. & Baren, B. (1992). Photothermal description of polymer ablation: Absorption behavior and degradation time scales. *J. Appl. Phys.* **72**, 5172–5178.

Duley, W.W. (1996). *UV Lasers Effects and Applications in Material Science*. Cambridge, UK: Cambridge University Press.

Fernandez, J.C., Hegelich, B.M., Cobble, J.A., Flippo, K.A., Letzring, S.A., Johnson, R.P., Gautier, D.C., Shimada, T., Kyrala, G.A., Wang, Y.Q., Wetteland, C.J. & Schreiber, J. (2005). Laser-ablation treatment of short-pulse laser targets:


https://doi.org/10.1017/S0263034607070231 Published online by Cambridge University Press

Towards an experimental program on energetic-ion interactions with dense plasmas. *Laser Part. Beams* **23**, 267–273.

Gamaly, E.G., Luther-Davies, B., Kolev, V.Z., Madsen, N.R., Duering, M. & Rode, A.V. (2005). Ablation of metals with picosecond laser pulses: Evidence of long-lived nonequilibrium surface states. *Laser Part. Beams* **23**, 167–176.

Gaponov, A.V., Lomov, A.S., Osipio, V. & Rabinovich, M.I. (1989). *Dynamics and evolution in non-linear waves*. Heidelberg: Springer.

Haken, H. (1978). *Synergetics: An Introduction, Nonequilibrium Phase Transitions and Self-Organization in Physics, Chemistry, and Biology*. Heidelberg: Springer.

Himmelbaur, M., Arnold, N., Yaren, B., Bityurin, N., Arenholz, E. & Baüerle, D. (1997). UV-laser-induced periodic surface structures on polymide. *Appl. Phy. A* **64**, 451.

Huadong, G. & Gregory, A.V. (1992). A computer simulation method for studying the ablation of polymer surfaces by ultraviolet laser radiation. *J. Appl. Phys.* **71**, 1415–1420.

Jarad, F.A., Durrani, S.M.A. & Islam, M.A. (1993). $CO_2$ pulsed laser effect on CR-39 registration properties. *Nucl. Inst. Meth. B* **74**, 419–425.

John, C.M. & Haglund, R.F., Jr. (1998). *Laser Ablation and Desorption*. New York: Academic Press.

Korero, G. (1988). Plume temperature in the laser ablation of polyimide films measured by infrared emission spectroscopy. *Appl. Phys. B* **46**, 147.

Kukreja, L.M. & Hess, P. (1994). Time evolution of laser-induced polymer ablation studied by attenuation of a probe HeNe laser beam. *Appl. Surf. Sci.* **79–80**, 158–164.

Kukreja, L.M. (1991). Studies on laser-induced irreversible surface softening in a thermoset polymer of allyl diglycol carbonate (CR-39) *J. Appl. Polymer Sci.* **42**, 115–125.

Miotello, A., Kelly, R., Braren, B. & Otis, C.E. (1992). Novel geometrical effects observed in debris when polymers are laser sputtered. *Appl. Phys. Letts.* **61**, 2784–2786.

Nakai, T., Hattori, K., Okano, A., Richard, N.I. & Haglund, F., Jr. (1991). Nonthermal laser sputtering from solid surfaces. *Nucl. Inst. Meth. B* **58**, 452–462.

Nicolis, G. & Prigogine, I. (1977). *Self-Organization in Non-Equilibrium Systems*. New York: John Wiley & Sons.

Nivis, Y., Piereux, J.J., Brezini, A., Petit E., Caudano, R., Lutgen, P., Feyder, G. & Lazare, S. (1998). Structural origin of surface morphological modifications developed on poly (ethylene terephthalate) by excimer laser photoablation. *J. Appl. Phys.* **64**, 365–370.

Page, J.B., Jr. (1974). Defect induced resonance modes in asymptotic limit of low frequencies: Isotope effects and amplitude patterns. *Phys. Rev. B* **10**, 719–738.

Rafique, M.S., Khaleeq-ur-Rahman, M., Khurram Siraj, M.S.A., Faryaal, M. & Afshan, A. (2005). Angulr distribution and forward peaking of laser produced plasma ions. *Laser Part. Beams* **23**, 131–135.

Rubhn, H.G. (1999). *Laser Applications in Surface Science Technology*. London: John Wiley & Sons.

Schade, W., Bohling, C., Hohmann, K. & Scheel, D. (2006). Laser-induced plasma spectroscopy for mine detection and verification. *Laser Part. Beams* **24**, 241–247.

Shahid, S., Rafique, M.S., Khaleeq-ur-Rahman, M., Ghauri, I.M. & Faizan ul-Haq. (2004). Effect of $CO_2$ laser irradiation on the track registration properties of CR-39. http://www.epsppd.epfl.ch/London/pdf/P5_045.pdf.

Sirinivasan, R. (1993). Ablation of polyimide (Kapton$^{TM}$) films by pulsed (ns) ultraviolet and infrared (9.17 $\mu$m) lasers. *Appl. Phys. A* **56**, 417–423.

Sirinivasan, R., Braren, B. & Kelly, G. (1990). Nature of "incubation pulses" in the ultraviolet laser ablation of polymethyl methacrylate *J. Appl. Phy.* **68**, 1842–1847.

Sumiyoshi, T., Nioimiya, Y., Ogasawara, H., Obara, M.A. & Tanaka, H. (1994). Efficient ablation of organic polymers polyether sulphone and polyether ether ketone by a TEA $CO_2$ laser with high perforation ability. *Appl. Phys. A* **58**, 475–479.

Sutcliffe, E. & Srinivasan, R. (1986). Dynamics of UV laser ablation of organic polymer surfaces. *J. Appl. Phys.* **60**, 3315.

Thareja, R.K. & Sharma, A.K. (2006). Reactive pulsed laser ablation: Plasma studies. *Laser Part. Beams* **24**, 311–320.

Trusso, S., Barletta, E., Barreca, F., Fazio, E. & Neri, F. (2005). Time resolved imaging studies of the plasma produced by laser ablation of silicon in $O_2$/Ar atmosphere. *Laser Part. Beams* **23**, 149–153.

Veiko, V.P., Shakhno, E.A., Smirnov, V.N., Miaskovski, A.M. & Nikishin, G.D. (2006). Laser-induced film deposition by LIFT: Physical mechanisms and applications. *Laser Part. Beams* **24**, 203–209.

Wieger, V., Strassl, M. & Wintner, E. (2006). Pico- and microsecond laser ablation of dental restorative materials. *Laser Part. Beams* **24**, 41–45.

Zweig, A.D. & Deutsch, T.F. (1992). Shock waves generated by confined XeCl excimer laser ablation of polyimide. *Appl. Phys. B* **54**, 76–82.